Modelling the catabolic environment of the moderately degenerated disc with a caprine ex vivo loaded disc culture system

RUSTENBURG, C.M.E., SNUGGS, J.W., EMANUEL, K.S., THORPE, Abbey, SAMMON, Chris <http://orcid.org/0000-0003-1714-1726>, LE MAITRE, Christine <http://orcid.org/0000-0003-4489-7107> and SMIT, T.H.

European Cells and Materials Vol. 40 2020 (pages 21-37) DOI: 10.22203/eCM.v040a02 ISSN 1473-2262

MODELLING THE CATABOLIC ENVIRONMENT OF THE MODERATELY DEGENERATED DISC WITH A CAPRINE *EX VIVO* LOADED DISC CULTURE SYSTEM

C.M.E. Rustenburg[1,§], J.W. Snuggs[2,§], K.S. Emanuel[1,5], A. Thorpe[2], C. Sammon[3], C.L. Le Maitre[2,*] and T.H. Smit[1,4]

[1] Amsterdam UMC, University of Amsterdam, Department of Orthopaedic Surgery, Amsterdam Movement Sciences, Amsterdam, the Netherlands
[2] Biomolecular Sciences Research Centre, Sheffield Hallam University, Sheffield, UK
[3] Materials and Engineering Research Institute, Sheffield Hallam University, Sheffield, UK
[4] Amsterdam UMC, University of Amsterdam, Department of Medical Biology, Amsterdam Movement Sciences, Amsterdam, the Netherlands
[5] Maastricht University Medical Center, Department of Orthopedic Surgery, Maastricht, the Netherlands
[§] These authors contributed equally to this work

Abstract

Low-back pain affects 80 % of the world population at some point in their lives and 40 % of the cases are attributed to intervertebral disc (IVD) degeneration. Over the years, many animal models have been developed for the evaluation of prevention and treatment strategies for IVD degeneration. *Ex vivo* organ culture systems have also been developed to better control mechanical loading and biochemical conditions, but a reproducible *ex vivo* model that mimics moderate human disc degeneration is lacking. The present study described an *ex vivo* caprine IVD degeneration model that simulated the changes seen in the nucleus pulposus during moderate human disc degeneration.

Following pre-load under diurnal, simulated physiological loading (SPL) conditions, lumbar caprine IVDs were degenerated enzymatically by injecting collagenase and chondroitinase ABC (cABC). After digestion, IVDs were subjected to SPL for 7 d. No intervention and phosphate-buffered saline injection were used as controls. Disc deformation was continuously monitored to assess disc height recovery. Histology and immunohistochemistry were performed to determine the histological grade of degeneration, matrix expression, degrading enzyme and catabolic cytokine expression.

Injection of collagenase and cABC irreversibly affected the disc mechanical properties. A decrease in extracellular matrix components was found, along with a consistent increase in degradative enzymes and catabolic proteins [interleukin (IL)-1β, -8 and vascular endothelial growth factor (VEGF)]. The changes observed were commensurate with those seen in moderate human-IVD degeneration. This model should allow for controlled *ex vivo* testing of potential biological, cellular and biomaterial treatments of moderate human-IVD degeneration.

Keywords: Intervertebral disc, loaded disc culture system, goat, disease model, moderate disc degeneration.

***Address for correspondence**: Prof. Christine Le Maitre, Biomolecular Sciences Research Centre, Sheffield Hallam University, City Campus, Howard Street, Sheffield S1 1WB, UK.
Email: C.Lemaitre@shu.ac.uk

List of abbreviations

AF	annulus fibrosus
ADAMTS4	a disintegrin-like and metalloprotease with thrombospondin type 1 motif 4
BSA	bovine serum albumin
cABC	chondroitinase ABC
DAB	3,3'-diaminobenzidine tetrahydrochloride
DMEM	Dulbecco's modified Eagle medium
FBS	foetal bovine serum
HEPES	4-(2-hydroxyethyl)-1-piperazineethanesulphonic acid
IDD	IVD degeneration
IHC	immunohistochemistry

IL	interleukin
IQR	interquartile range
IVD	intervertebral disc
LBP	low-back pain
LDCS	loaded disc culture system
MMP3	matrix metalloproteinase 3
NGF	nerve growth factor
NP	nucleus pulposus
PBS	phosphate-buffered saline
SD	standard deviation
TBS	tris-buffered saline
TNFα	tumour necrosis factor α
VEGF	vascular endothelial growth factor
YLDs	years lived with disability

Introduction

LBP is the leading cause of morbidity and YLDs worldwide (Vos *et al.*, 2017). Several causes have been related to LBP, the main being lumbar degeneration, which is thought to account for approximately 40 % of all LBP cases (de Schepper *et al.*, 2010; Pye *et al.*, 2004; van Tulder *et al.*, 1997). IVD degeneration is a process in which the healthy IVD follows a vicious cycle towards joint destruction (Vergroesen *et al.*, 2015).

The healthy IVD consists of two cartilaginous endplates that are attached to the adjacent vertebrae and confine the NP, which is the core of the IVD, and the AF, which encircles the NP (Shapiro *et al.*, 2012). The NP contains NP cells that produce a large amount of proteoglycans and collagen type II (Ohshima and Tsuji, 1989; Roberts *et al.*, 1991). Since proteoglycans are negatively charged, an osmotic pressure attracts water into the NP creating an intradiscal pressure (Ohshima and Tsuji, 1989). This causes tension in the collagen fibres of the AF and enables the IVD to withstand the high compressive forces imposed by gravity and muscle tension. The IDD is an irreversible process characterised by altered cell behaviour, loss of NP matrix and changed joint mechanics (Adams and Roughley, 2006; Weber *et al.*, 2015). This vicious circle of events can be initiated by various factors of both biological and mechanical nature (Vergroesen *et al.*, 2015). The alterations in cell biology and matrix turnover essentially leads to a fibrous NP, which can no longer sustain compressive loads and enhance structural and biomechanical failure, largely mediated by catabolic processes (Le Maitre *et al.*, 2015; Risbud and Shapiro, 2014; Vergroesen *et al.*, 2015; Vo *et al.*, 2016). Ultimately, IDD can result in spinal instability, with decreased disc height, tears and clefts in the degenerating AF and bulging of the disc into the spinal canal. The IVD loses its intradiscal pressure and the hydrostatic pressure experienced by NP cells switches to shear stress, which induce catabolic and inflammatory gene expression (Emanuel *et al.*, 2015; Iatridis *et al.*, 1997; Paul *et al.*, 2013). These changes lead to compression of neural tissues, neurovascular invasion of the disc and inflammation of the adjacent bone, all inducing chronic pain (Le Maitre *et al.*, 2015).

Patients suffering chronic LBP due to IDD, who have exhausted conservative treatment (*e.g.* pain relief medication and physiotherapy), have no remaining options other than surgical intervention, of which the most common is spinal fusion (Yajun *et al.*, 2010). However, in the last few years, a number of biological, cellular or biomaterial strategies have been developed that aim at the restoration of the IVD and offer promising *in vitro* results (Anderson *et al.*, 2005; Schutgens, 2015; Thorpe *et al.*, 2016; Thorpe *et al.*, 2017; Tsujimoto *et al.*, 2018). However, translation to clinic is currently limited by a lack of models that recapitulate the cellular and mechanical changes seen in human disc degeneration.

Tissue regeneration is essentially a biological process that requires a living IVD to evaluate safety and efficacy of interventions. Animal models have been developed and used for this purpose (Hoogendoorn *et al.*, 2007; Wei *et al.*, 2014; Wuertz *et al.*, 2009), but animal models have limitations of practical, ethical and mechanical nature. In the last decade, there has been a strong urge in science to limit the use of experimental animals, not only for ethical reasons, but also because animal models are often moderate to poor models of the human condition that is simulated. Reduction, replacement and refinement (3Rs) is a policy strongly embraced by grant agencies throughout the world. As for the validity of the model, quadrupeds have been presented as relevant for human spine research (Smit, 2002), but the diurnal loading regime and biology in humans is quite different from what is seen in a sheep or goat, making it difficult to predict the benefit of a treatment for humans. Finally, the induction of a relevant disc degeneration in the IVD of a quadruped is far from trivial. Puncture of the AF with a needle is often used, but essentially differs from normal disc degeneration in humans, which usually starts with the loss of proteoglycans and water from the NP. To simulate this, Hoogendoorn *et al.* (2007) have used cABC, inducing a reproducible, mild disc degeneration in a goat model, similarly to what was done by Gullbrand *et al.* (2017). However, in both studies, it took 12 weeks to produce these conditions. As such, this is an expensive and unpractical model for the evaluation of innovative treatments during early stage development.

To overcome these issues, LDCSs have been proposed and developed (Alini *et al.*, 2008; Gantenbein *et al.*, 2015; Lang *et al.*, 2018; Paul *et al.*, 2012; Pfannkuche *et al.*, 2019; Rosenzweig *et al.*, 2016; Walter *et al.*, 2014; Zhang *et al.*, 2020). As the disc is considered to be an immune-privileged site (Sun *et al.*, 2020), with inflammatory cell migration only seen following annular or endplate rupture during end stage degeneration or herniation, studies of isolated discs *ex vivo* can be appropriate models for testing potential regenerative strategies. IVDs are excised from sheep, cattle or goat spines or tails from a slaughterhouse and placed in a bioreactor. Such IVDs are generally in good condition and, therefore,

Table 1. Features of human disc degeneration.

Cellular changes during human disc degeneration	Reference	Method of measurement
Cellular clusters	Boos *et al.*, 2002; Gries *et al.*, 2000; Rutges *et al.*, 2013; Sive *et al.*, 2002	Histological examination
Fissures	Boos *et al.*, 2002; Gries *et al.*, 2000; Rutges *et al.*, 2013; Sive *et al.*, 2002	Histological examination
Demarcation between NP and AF	Boos *et al.*, 2002; Gries *et al.*, 2000; Rutges *et al.*, 2013; Sive *et al.*, 2002	Histological examination
Loss of matrix staining, particularly pericellular matrix within the NP	Boos *et al.*, 2002; Gries *et al.*, 2000; Rutges *et al.*, 2013; Sive *et al.*, 2002	Histological examination
Decreased matrix synthesis	Iatridis *et al.*, 1999; Korecki *et al.*, 2008; Le Maitre *et al.*, 2007; Roberts *et al.*, 2001; Roughley, 2004	IHC for classical NP matrix proteins: collagen type II and aggrecan
Increased matrix-degrading enzymes	Le Maitre *et al.*, 2007; Pockert *et al.*, 2009; Séguin *et al.*, 2006	IHC for MMPS and ADAMTs
Increased expression of catabolic cytokines by NP cells	Hoyland *et al.*, 2008; Le Maitre *et al.*, 2005; Phillips *et al.*, 2013	IHC for cytokines
Nerve ingrowth (driven by increased production of neurotrophic factors by NP cells)	Binch *et al.*, 2015; Lama *et al.*, 2018	IHC for neurotropic factors
Angiogenesis (driven by increased production of VEGF by NP cells)	Binch *et al.*, 2014; Doita *et al.*, 1996; Lama *et al.*, 2018; Rätsep *et al.*, 2013	IHC for VEGF
Decreased mechanical properties	Emanuel *et al.*, 2015; Korecki *et al.*, 2008; McMillan *et al.*, 1996; Walter *et al.*, 2011; Wang *et al.*, 2007; Wuertz *et al.*, 2009	In-line mechanical properties

offer a reproducible experimental environment. Well-defined mechanical studies have shown that regular diurnal loading is a prerequisite for the IVDs to stay healthy (Paul *et al.*, 2012), while overloading leads to the onset of disc degeneration, as characterised by increased catabolic and inflammatory gene expression (Paul *et al.*, 2013). However, this condition is only the start of disc degeneration and still far from a moderately degenerated human IVD, which is the target for regeneration studies. To obtain degenerate conditions, several methods have been used. The injection of trypsin and papain into bovine motion segments leads to a decrease in glycosaminoglycan content and cellularity within the NP (Roberts *et al.*, 2008). Walter *et al.* (2015) added TNFα to the culture medium to induce an inflammatory and degenerative reaction of the NP cells. Teixeira *et al.* (2015) used a similar strategy with the injection of IL-1β, while Paul *et al.* (2018) induced degeneration by injecting cABC. While such interventions are useful to study the onset and early events in IVD degeneration, they do not simulate the moderate degeneration at which interventions are targeted. Indeed, more severe degeneration is required and it needs to be obtained in a fast and reproducible way so that early stage therapies can be investigated in an economical and rapid manner. Therefore, the aim of the present study was to develop a fast and reproducible *ex vivo* model of moderate disc degeneration, which could be used as a short-term, isolated model system for the screening and evaluation of prospective prevention and treatment strategies, prior to long-term testing in an *in vivo* setting.

To this end, the study's hypothesis was that the injection of collagenase and cABC (col/cABC) would quickly degrade the matrix of the disc, providing an altered mechanical environment. In turn, this would induce an altered response to load, stimulating catabolic mediator (such as IL-1) production as well as leading to an increase in catabolic and inflammatory enzymes and a decrease in matrix synthesis and markers of native disc degeneration, hence mimicking the cellular processes seen in moderate human-disc degeneration (Table 1).

Materials and Methods

Optimisation of enzyme degradation

Prior to the *ex vivo* loading studies, the concentration of cABC and collagenase type II was determined. The spine of one skeletally mature milk goat (between 3 and 5 years old) was obtained from the local abattoir (Sheffield, UK). Thirteen IVDs were randomly assigned to the following treatment groups (cABC, C3667, Sigma-Aldrich; collagenase type II, 17101015, Gibco):

- non-injected control;
- PBS-injected control;
- 0.5 U/mL cABC;
- 1 U/mL cABC;
- 2 U/mL cABC;
- 1 mg/mL collagenase;
- 2 mg/mL collagenase
- 4 mg/mL collagenase;
- 1 mg/mL collagenase + 0.5 U/mL cABC;

- 1 mg/mL collagenase + 2 U/mL cABC;
- 2 mg/mL collagenase + 0.5 U/mL cABC;
- 2 mg/mL collagenase + 1 U/mL cABC;
- 4 mg/mL collagenase + 2 U/mL cABC.

The IVDs were injected as described above using a 29G needle and incubated for 2 h at 37 °C. Following digestion, the IVDs were isolated from the spine using a scalpel blade and fixed in 10 % v/v neutral-buffered formalin (Leica) and embedded in paraffin wax. 4 μm-thick sections were cut and mounted on to positively charged slides and stained histologically with haematoxylin and eosin, Masson's trichrome and alcian blue to determine the level of matrix degradation and identify the enzyme degradation methodology able to induce moderate degradation of the healthy IVD matrix. The IVDs were inspected for signs of matrix degradation (by two researchers, CLM and AT), namely presence of micro fissures and decreased proteoglycan and collagen staining, but whilst avoiding large defects or voids within the disc space. Microscopical images were captured to document changes.

Caprine samples and IVD isolation

Nine lumbar spines from skeletally mature female Dutch milk goats (3-5 years old) were obtained from a local abattoir (Amsterdam, the Netherlands). The spines were sterilised using medical grade iodide-alcohol solution. Within 24 h after slaughter, the excessive soft tissue and muscles were removed and the IVDs with adjacent cartilaginous endplates were dissected in two parallel planes using an oscillating surgical saw, all under sterile conditions. Once dissected, the IVDs (n = 33) were cleaned using sterile gauzes to remove muscle or ligament tissue and rinsed in PBS and 70 %v/v ethanol to remove sawing debris.

LDCS

The LDCS consists of individual culture chambers that are placed in an incubator at 37 °C (Paul *et al.*, 2012). The total culture period of the IVDs was 10 d and the IVDs were cultured in standard DMEM (Gibco) supplemented with 10 % FBS (HyClone), 4.5 g/L glucose (Merck), 25 mmol/L HEPES (Invitrogen), 50 μg/mL ascorbate-2-phosphate (Sigma-Aldrich,), 10,000 U/mL penicillin, 10 mg/mL streptomycin and 25 μg/mL amphotericin B (Gibco). Each culture chamber contained 50 mL of culture medium that circulated continuously at the velocity of 3 mL/h by using a peristaltic pump. Medium was changed every 3-4 d, after flushing using 25 mL of PBS per culture chamber.

During the whole culture period, the IVDs were loaded with dynamic axial loading consisting of simulated physiological loading (Paul *et al.*, 2012). This loading pattern started with 16 h of a sinusoidal load of 1 Hz that alternated in magnitude every 30 min (between 0.09-0.11 MPa and 0.1-0.6 MPa), followed by 8 h of a low sinusoidal load of 1 Hz (0.09-0.11 MPa), reflecting loading magnitudes and frequency derived from *in vivo* measurements of pressure in a goat lumbar spine (Paul *et al.*, 2012).

Degeneration

After 3 d of pre-loading with simulated physiological loading to establish dynamic equilibrium, loading was paused and culture chambers were removed from the LDCS. The IVDs (n = 33) were randomly divided into three experimental groups to ensure disc levels and animals were mixed into the groups to account for biological variance:

- no injection (*i.e.* control group; n = 9);
- injection with PBS (n = 12);
- injection with 1 mg/mL collagenase and 2 U/mL cABC (n = 12).

The IVDs were removed from their culture chamber under sterile conditions and injected using a 29G needle with 50 μL of 1 mg/mL collagenase and 2 U/mL cABC or PBS, as appropriate. Following injection, the IVDs were placed back into their individual culture chamber and in the LDCS again. Following 2 h digestion, fresh medium was applied and the IVDs were subjected to simulated physiological loading, as described above, for 7 d.

Biomechanical data analysis

Changes in disc height were measured using an OADM 12U6430/S35A optoelectric sensor (Baumer, Berlin, Germany) and a Kam-e load cell K-1613 (Bienfait, Haarlem, the Netherlands) measured the forces applied on to the disc. Signals were digitised at 100 Hz. Customised programs in MATLAB (MathWorks) were used for data analysis. To investigate biomechanical properties, outcome parameters included disc height loss over time, time constants of axial decompression and stiffness per day. To calculate disc height changes, the disc height at the end of the final day was subtracted from the disc height at the end of the first day after injection. Time constants were calculated by fitting of a stretched exponential on the recovery data (van der Veen *et al.*, 2007):

$$\delta(t) = \delta_\infty(1 - e^{\left(-\left(\frac{t}{\tau}\right)^{\beta}\right)})$$

Where δ is the change in disc height in mm; t is time; $\delta\infty$ is the disc height at equilibrium; τ is the time constant; β is the stretch constant.

The quality of fit was checked by visual inspection and linear regression analysis with a cut off of R2 > 0.98 for analysis, which was always the case. Stiffness was calculated by dividing the amplitude of the force signal by the amplitude of the disc height signal during the final high load phase of the day (Emanuel *et al.*, 2015).

Determination by histology and IHC of degeneration induction as compared to human disc degeneration

Following completion of loading in the LDCS for 10 d (*i.e.* 3 d pre-load and 7 d post-enzyme digestion), the IVDs were removed from their culture chamber and fixed in 10 % neutral-buffered formalin for 1 week and, thereafter, decalcified for 1 week using Decalcifier II (Leica). ~ 3 mm-thick tissue slices were cut paramidsagittally from the IVD using a scalpel and embedded in paraffin wax. Thin slices (4 μm) were cut and mounted onto positively charged slides (Leica). The extent of histological disc degeneration was determined by histological grading commonly utilised to assess the degree of human disc degeneration, namely investigating key features of demarcation, fissures, loss of matrix staining and cellular clusters (Fig. 1; Table 1) following haematoxylin and eosin, Masson's trichome and alcian blue stainings (Le Maitre *et al.*, 2004; Sive *et al.*, 2002). IHC was used to assess the characteristic proteins that change during human disc degeneration (Table 1) in order to determine the cellular changes induced by degradation in goat discs as compared to the gold standard (human disc degeneration). Proteins representative of matrix, matrix degrading enzymes, key cytokines and factors that *in vivo* lead to nerve and blood vessel ingrowth were investigated: collagen type II, aggrecan, MMP3, ADAMTS 4, IL-1β, IL-8, VEGFA and NGF, as described previously (Le Maitre *et al.*, 2005; Thorpe *et al.*, 2016). Briefly, tissue sections were de-waxed in Sub-X Clearing Medium (Leica) and rehydrated in industrial methylated spirit (IMS; Sigma-Aldrich). Endogenous peroxidases were blocked for 30 min at room temperature in IMS containing 3 % (v/v) H_2O_2 (Sigma-Aldrich). Antigen retrieval was performed by incubating the slides for 30 min at 37 °C in TBS (20 mM tris, 150 mM NaCl, pH 7.5) containing 0.1 % (w/v) $CaCl_2$ and 0.01 % (w/v) α-chymotrypsin (Sigma-Aldrich). Following antigen retrieval, slides were blocked for 1 h at room temperature in TBS containing 1 % (w/v) BSA and 25 % (v/v) serum (rabbit or goat, Abcam, matched to the host species of the secondary antibody) before primary antibody incubation overnight at 4 °C: collagen type II (1 : 100, ab3092), aggrecan (1 : 200, ab3778), MMP3 (1 : 400, ab53015), ADAMTS4 (1 : 200, ab185722), IL-1β (1 : 100, ab53732), IL-8 (1 : 200, ab106350), VEGFA (1 : 100, ab52917) and NGF (1 : 100, ab52918) (all Abcam). All antibodies were diluted in TBS containing 1 % (w/v) BSA. IgG controls were used in the place of

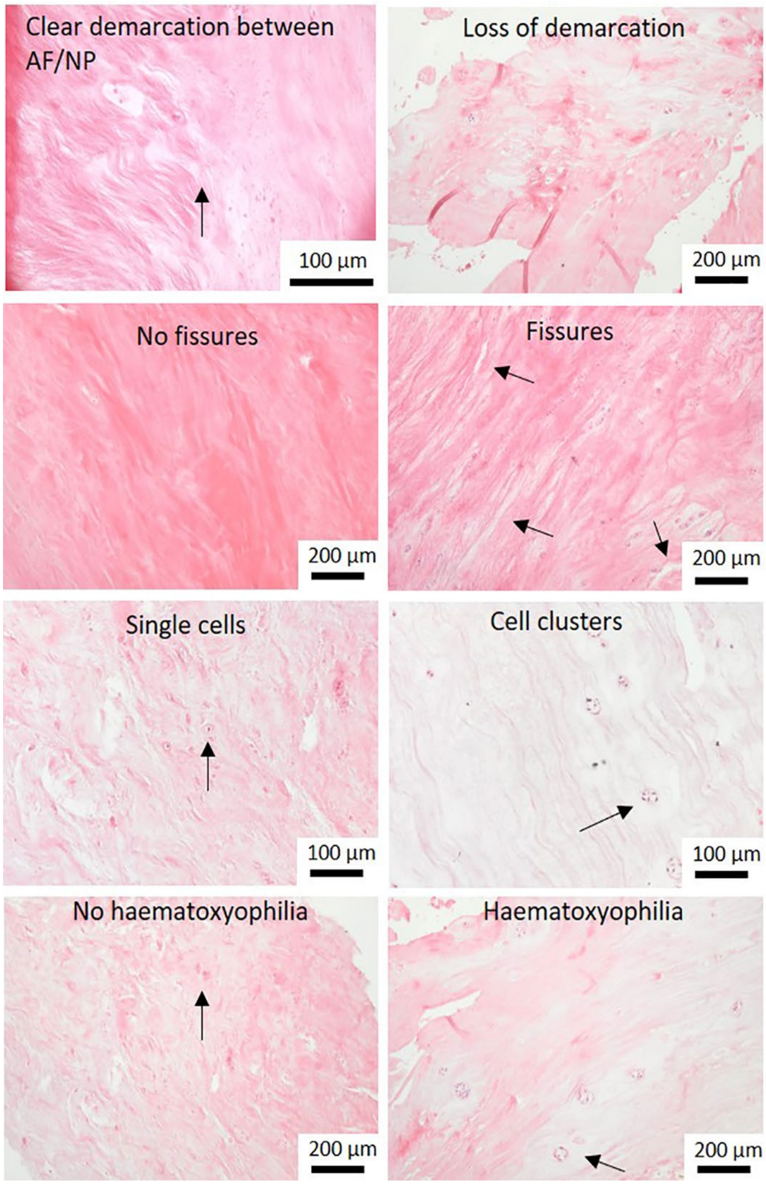

Fig. 1. Histological features of human degenerations utilised for histological grading.

primary antibodies at equal protein concentrations (mouse IgG control: ab170190; rabbit IgG control: ab37415; Abcam). Following washes in TBS, slides were incubated with biotinylated secondary antibody (1 : 500, goat anti-rabbit, ab6720 or 1 : 500, rabbit anti-mouse, ab7074, Abcam). Antibody binding was detected by adding VECTASTAIN® Elite ABC-HRP Kit, Peroxidase (Vector Laboratories) for 30 min at room temperature before incubation for 20 min at room temperature with TBS containing 0.08 % (v/v) H_2O_2 and 0.65 mg/mL DAB (Sigma-Aldrich). Nuclei were counterstained using Mayer's haematoxylin (Leica) and sections were finally dehydrated in IMS, cleared in Sub-X Clearing Medium and mounted using Mounting Medium Pertex® Histolab (Leica). Slides were visualised using an Olympus BX60 microscope and images captured using CellSens software (Olympus). Analysis was restricted to morphologically distinct NP tissue: an area of NP tissue was identified histologically and cells were counted using a panning method to ensure regions were not double counted. To avoid selection bias, all cells within the field of view were counted as immunopositive (brown) or immunonegative (purple nuclei only) until a total of 200 NP cells had been counted. Then, percentage immunopositivity for NP cells was determined.

Statistics

The assumption of normality of the biomechanical data was checked by visual inspection of histograms, Q-Q plots and box plots of the data within the groups.

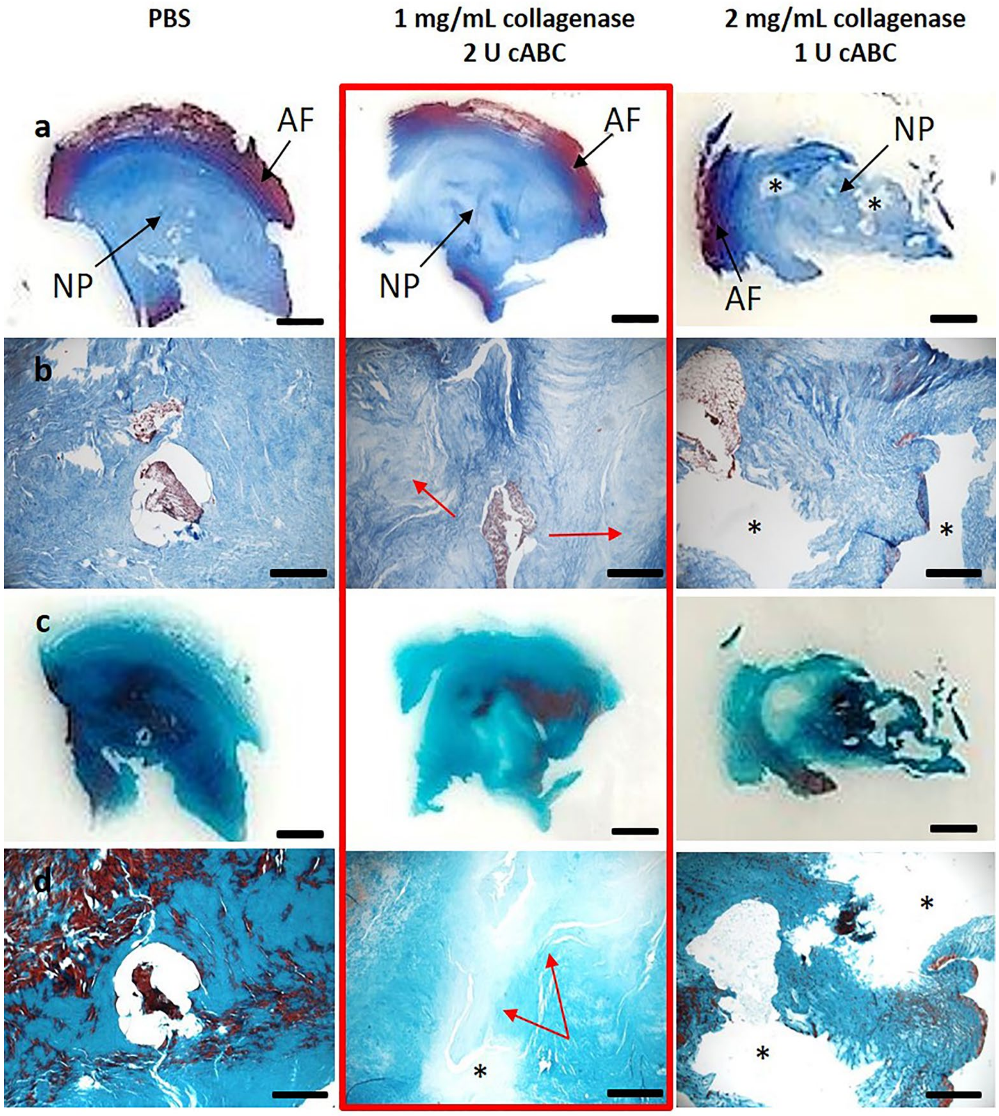

Fig. 2. Enzyme degradation optimisation. Caprine IVDs were injected with different concentrations and combinations of collagenase and cABC and histologically stained with (**a**,**b**) Masson trichrome and (**c**,**d**) alcian blue to detect collagen and glycosaminoglycan deposition, respectively, within the IVDs. More than 1 mg/mL collagenase destroyed the NP tissue, whereas 1 mg/mL collagenase combined with 2 U cABC induced mild degradation of the collagens and proteoglycans in the disc whilst preserving overall tissue structure. This was chosen as the optimised degenerative treatment (red box). PBS was injected into caprine IVDs as a control. (**a**,**c**) Scale bar: 500 μM. (**b**,**d**) Scale bar: 100 μM. Red arrows indicate regions of decreased matrix staining, Asterisks indicate tissue destruction.

Shapiro-Wilks tests were also performed on the data. To test whether the biomechanical data appeared to be normally distributed, a one-way ANOVA on the effect of treatment group with *post-hoc* Bonferroni correction was applied. Kruskal-Wallis tests were used to test for differences in time constants, with *post-hoc* Mann-Whitney U test for differences between the three groups. IHC immunopositivity data was not normally distributed and, thus, a Kruskall-Wallis with Dwass-Steel-Critchlow-Fligner *post-hoc* analysis test was used to identify significant differences in immunopositivity across treatment groups. Statistical tests were performed using SPSS (IBM Software, Armonk NY, USA, version 20 for Windows) or Stats Direct (Warrington, UK). A $p < 0.05$ was considered statistically significant.

Results

Optimisation of enzyme degradation

The IVDs accepted a maximum injection volume of 50 μL. In all treatments, the outer AF was maintained, however, the highest concentration of enzymes applied to the IVDs obliterated the NP. Where collagenase concentrations exceeded 1 mg/mL, destruction of the NP was noted (Fig. 1). Thus, such concentrations were deemed not suitable for further testing within the LDCs. However, at 1 mg/mL of collagenase most of the tissue was intact, although fissures were observed in the AF, mimicking those seen during human disc degeneration, whilst at 0.5 mg/mL only limited fissures were seen. cABC treatments did not induce major defects within the tissue but displayed decreased alcian blue staining in a dose-dependent manner (Fig. 2). Following visual inspection, both researchers (CLM and AT) noted that the combination of 1 mg/mL collagenase and 2 U/mL cABC (col/cABC) induced features similar to those seen during histological examination of human discs, mimicking a moderate degradation of collagens and proteoglycans in the disc whilst preserving overall tissue structure, with the presence of small fissures in the NP and AF (Fig. 2).

Biomechanical evaluation

The injection of cABC and collagenase decreased the mechanical stability of the IVDs, especially in diurnal creep behaviour (Fig. 3). Disc height decreased progressively over time, whereas control and PBS-injected groups remained in stable dynamic equilibrium over the duration of the culture period. The mean ± SD loss of disc height between day 1 and 5 after injection was 0.278 ± 0.16 mm, significantly more when compared to 0.029 ± 0.019 mm ($p < 0.001$) in the control group and 0.036 ± 0.034 mm ($p < 0.001$) in the PBS group (Fig. 3). No difference was found between the control and PBS group ($p = 1.00$). There was also an increase in time constant 5 d after injection (median τ = 5.95 h; IQR: 5.10, 10.47) when compared to the final day before injection (median τ = 3.75 h; IQR: 3.24, 6.28; p = 0.002) for the enzyme-injected discs (Table 2). This was also significantly increased when compared to control (median τ = 3.18 h; IQR: 2.39, 5.94; p = 0.011) and PBS groups (median τ = 2.60 h; IQR: 2.12, 3.44; p = 0.002), which did not differ from each other significantly (p = 0.394). No significant changes in stiffness were found after cABC and collagenase injection when compared to non-injected ($p = 0.657$), and PBS-injected discs ($p = 0.136$) (Fig. 3).

Morphological appearance and histological grading

The average histological grade of enzyme-injected IVDs (6.2 ± 0.84), with the presence of fissures, demarcation, cell clusters and loss of pericellular matrix (Fig. 4) indicated that these discs showed features similar to moderately degenerated human discs, whereas the average histological grades of non-injected (2.9 ± 0.96) and PBS-injected (2.6 ± 1.65) control IVDs indicated features similar to non-degenerate human discs. Masson's trichrome and alcian blue staining demonstrated that enzyme-injected discs displayed lower levels of healthy extracellular matrix as compared to non-injected and PBS-injected controls (Fig. 4).

Matrix synthesis

Following treatment and culture within the LDSC, the number of NP cells in enzyme-injected caprine

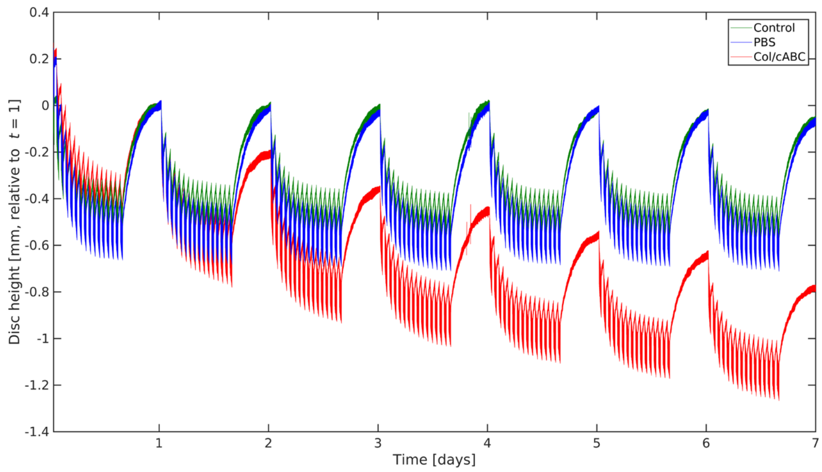

Fig. 3. Diurnal creep behaviour of the IVDs. Control, non-injected discs (green) and PBS-injected discs (blue) showed immediate equilibrium, whereas the cABC- and collagenase-injected discs showed decreasing creep behaviour.

Table 2. Median (Q1, Q3) values of the time constants and mean ± SD values of loss of disc height between day 1 and 5 after injection.

	Time constants of pre-load day 3	Time constants of treatment day 1	Time constants of treatment day 5	Change in disc height between treatment day 1 and 5
Control	4.03 (2.61, 4.96)	3.19 (2.66, 5.67)	3.18 (2.39, 5.94)	0.029 ± 0.02
PBS	3.36 (2.91, 5.47)	3.10 (2.23, 5.60)	2.60 (2.12, 3.44)	0.036 ± 0.03
Coll/cABC	3.75 (3.24, 6.28)	4.59 (3.33, 7.79)	5.95 (5.10, 10.47)	0.278 ± 0.16

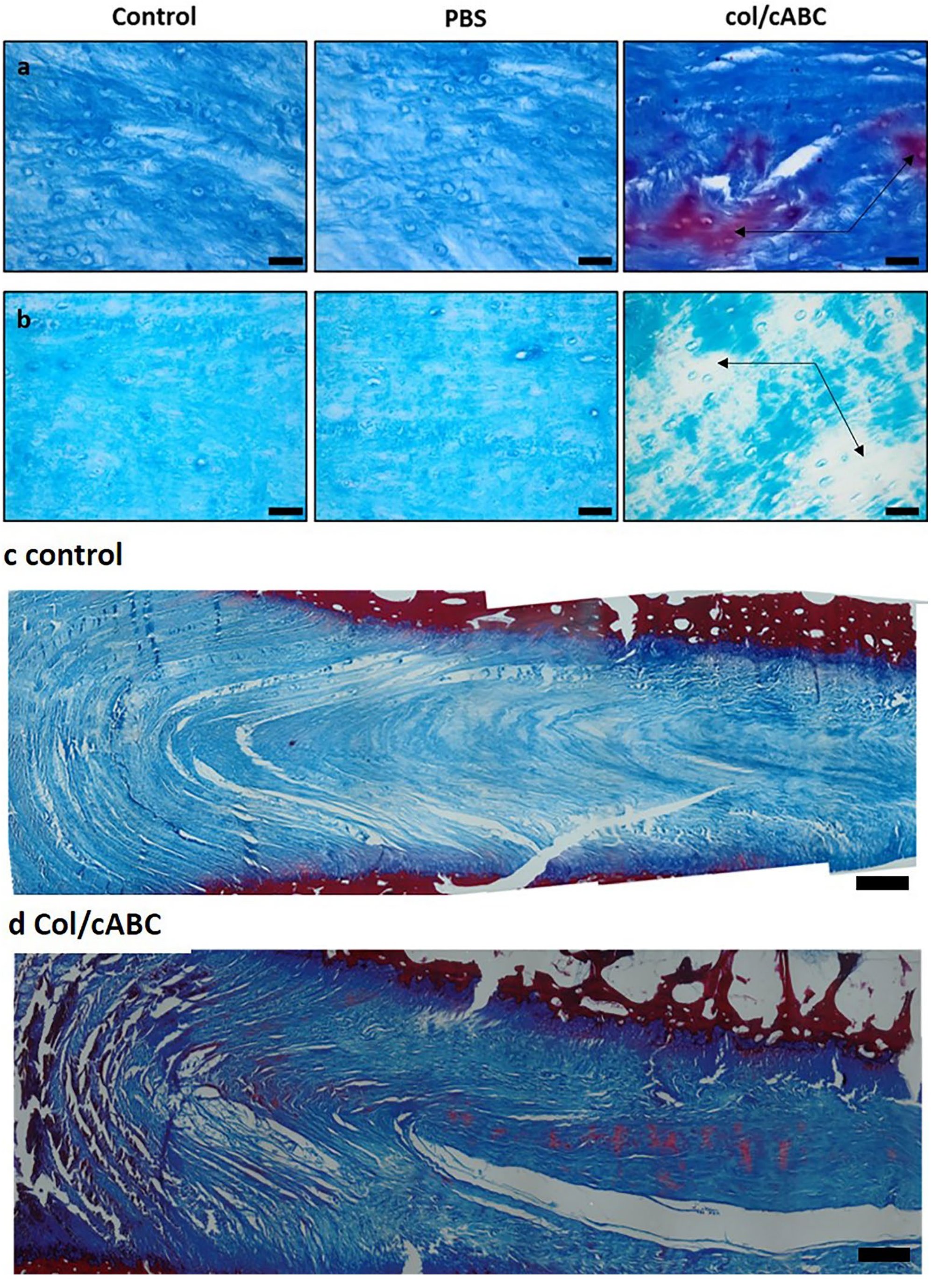

Fig. 4. Matrix deposition within no-injection (control), PBS-injected (PBS) and enzyme-injected (col/cABC) IVDs. (**a**) Masson trichrome staining highlighted collagen deposition and (**b**) alcian blue staining glycosaminoglycans within the extracellular matrix of the NP tissue. Scale bar: 50 µm. (**c**,**d**) Microscopically tiled image of control and enzyme-injected discs stained with Masson's trichrome to demonstrate matrix destruction in enzyme-injected degenerate discs. Scale bar: 500 µm.

IVDs expressing collagen type II was significantly reduced when compared to non-injected ($p = 0.022$) and PBS-injected ($p = 0.027$) IVDs (Fig. 5). The number of NP cells expressing aggrecan was also significantly decreased in enzyme-injected IVDs as compared to non-injected ($p = 0.024$) and PBS-injected ($p = 0.025$) IVDs (Fig. 5, isotype controls Fig. 7).

Catabolic enzyme and cytokine expression

The number of NP cells expressing proteins associated with IVD degeneration – MMP3 (no-injection *vs.* enzyme $p = 0.01$; PBS *vs.* enzyme $p = 0.038$), ADAMTS4 (no-injection *vs.* enzyme $p = 0.014$; PBS *vs.* enzyme $p = 0.029$), IL-1β (no-injection *vs.* enzyme $p = 0.006$; PBS *vs.* enzyme $p = 0.038$), IL-8 (no-injection *vs.* enzyme $p = 0.043$; PBS *vs.* enzyme $p = 0.018$) and VEGFA (no-injection *vs.* enzyme $p = 0.028$; PBS *vs.* enzyme $p = 0.006$) – was significantly increased in enzyme-injected discs when compared to non-injected and PBS-injected discs (Fig. 5,6; isotype controls Fig. 7). The proportion of NP cells expressing NGF was slightly increased in enzyme-injected discs when compared to non-injected and PBS-injected discs, despite not significantly (no-injection *vs.* enzyme $p = 0.064$; PBS *vs.* enzyme $p = 0.161$).

Discussion

The study aimed to develop a fast, reproducible *ex vivo* model for disc degeneration representing the phenotype seen during moderate human degeneration and usable as a disease model for testing regenerative therapeutics such as biologics, biomaterials or cell therapies. The data presented demonstrated that injection of 50 μL of 1 mg/mL collagenase and 2 U/mL cABC into healthy, caprine IVDs, followed by application of dynamic biomechanical loading for 7 d, induced a cellular phenotype with decreased matrix synthesis (collagen II, aggrecan) and increased production of catabolic enzymes (MMP3, ADAMTS4), cytokines and

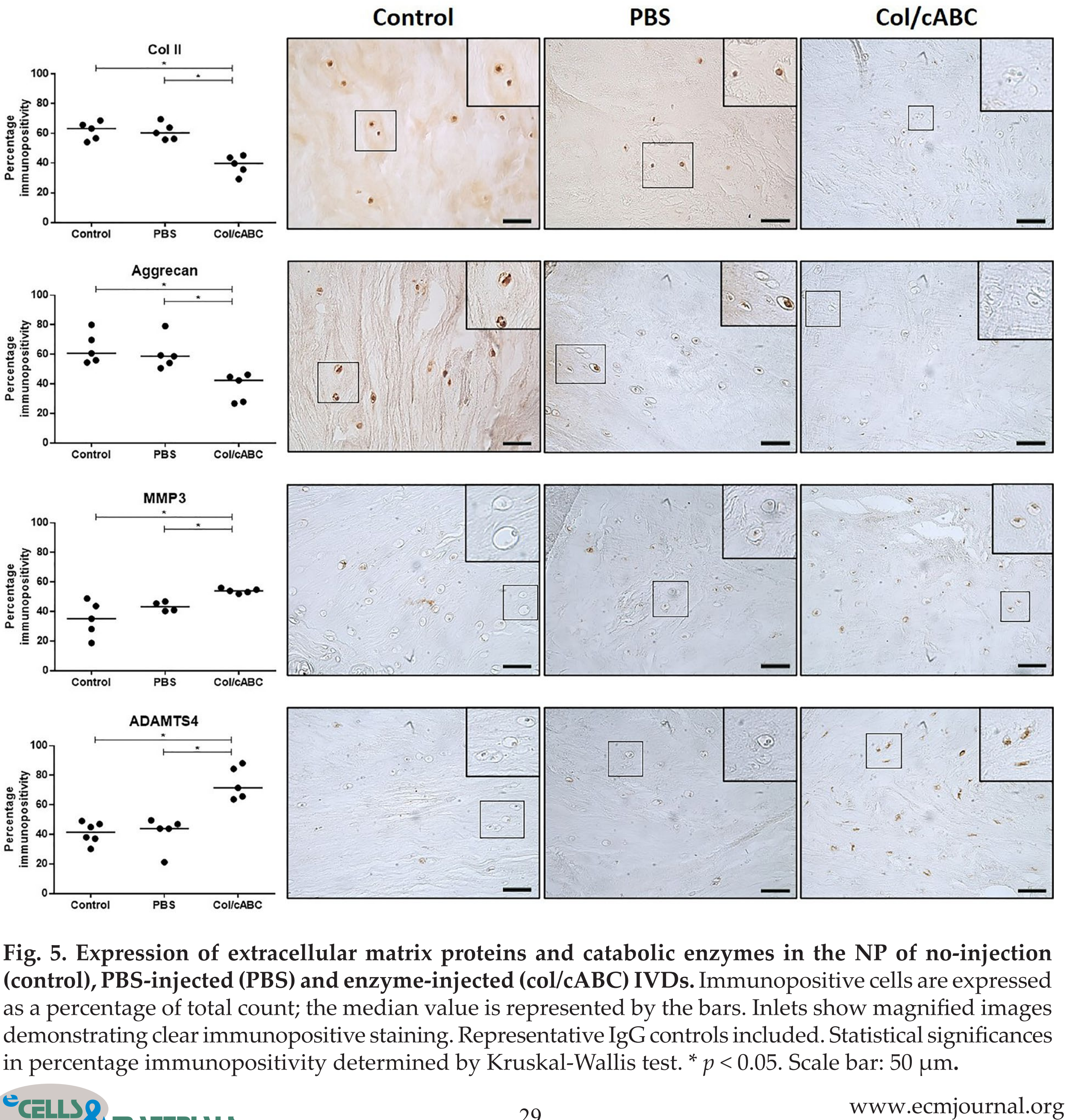

Fig. 5. Expression of extracellular matrix proteins and catabolic enzymes in the NP of no-injection (control), PBS-injected (PBS) and enzyme-injected (col/cABC) IVDs. Immunopositive cells are expressed as a percentage of total count; the median value is represented by the bars. Inlets show magnified images demonstrating clear immunopositive staining. Representative IgG controls included. Statistical significances in percentage immunopositivity determined by Kruskal-Wallis test. * $p < 0.05$. Scale bar: 50 μm.

growth factors (IL-1β, IL-8, VEGFA), thus mimicking the features seen during moderate human disc degeneration. Furthermore, altered biomechanical behaviour of the IVDs was observed with increased time constants and decreased creep behaviour over time.

The changes observed in biomechanical properties are similar to those seen previously in moderate IVD degeneration in humans (Emanuel *et al.*, 2015). In a similar *ex vivo* loaded disc culture system, Emanuel *et al.* (2015) have investigated the mechanical response of human IVDs with mild to end-stage degeneration, based on Pfirrmann-score (Pfirrmann *et al.*, 2001), to diurnal load. In moderately degenerated discs (*i.e.* Pfirrmann grade 3), there was less subsidence during a day of loading and a lower subsidence rate at the end of the day, with higher stiffness, as compared to a less degenerated disc. These changes were even more distinct in severely degenerated discs (*i.e.* Pfirrmann grade 4 and 5) (Emanuel *et al.*, 2015). Overall, the alterations in mechanical behaviour in the *ex vivo* caprine IVD model were reflected by the changes identified in the extracellular matrix, as seen by histological staining and grading, thereby demonstrating the induction of moderate degeneration.

Preclinical models of disc degeneration are essential tools to evaluate safety and efficacy of new clinical treatments. To mimic the disease as much as possible, it is important to take characteristic features of the human IVD into account, such as the absence of notochordal cells in human discs and the size of the animal disc relative to the human disc (Daly *et al.*, 2016; Thorpe *et al.*, 2018). Since the IVDs of goats do not contain notochordal cells (Hoogendoorn, 2009), have the same proportions as human discs (albeit 2-fold smaller) (Krijnen *et al.*, 2006) and are mainly loaded by axial compression (Smit, 2002), the caprine IVD is an acceptable representative model of the human IVD, maybe more so than

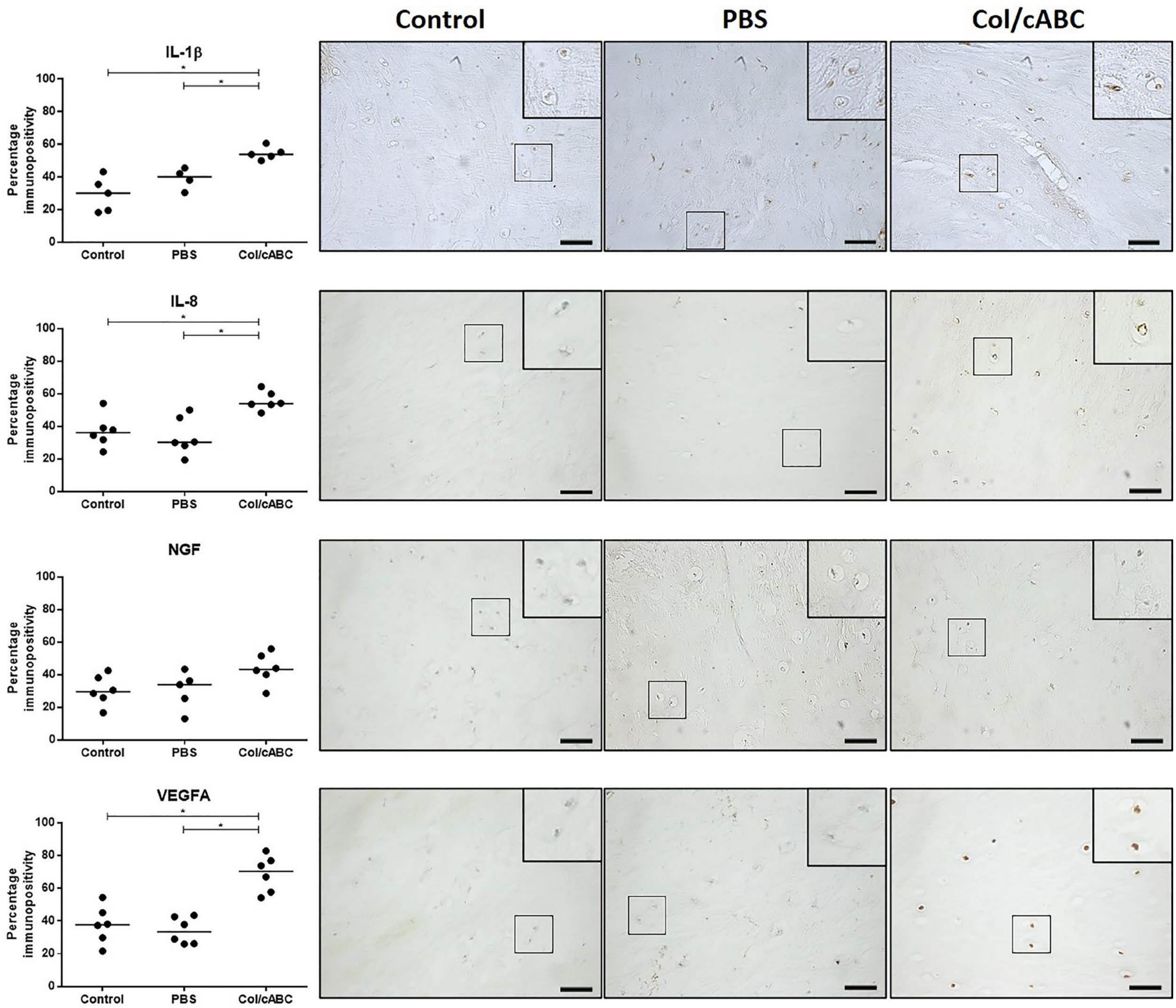

Fig. 6. Expression of catabolic proteins associated with IVD degeneration in the NP of no-injection (control), PBS-injected (PBS) and enzyme-injected (col/cABC) IVDs. Immunopositive cells are expressed as a percentage of total count; the median value is represented by the bars. Inlets show magnified images demonstrating clear immunopositive staining. Statistical significances in percentage immunopositivity determined by Kruskal-Wallis test * $p < 0.05$. Scale bar: 50 μm.

other models that are much smaller (murine, rat) or have much lower disc height (porcine) and contain notochordal cells (Daly *et al.*, 2016). The use of an *ex vivo* rather than an *in vivo* model allows for a better control of boundary conditions, including nutrient supply and mechanical loading conditions, as well as the characterisation of the mechanical properties of the healthy and degenerated discs. At the same time, it should be recognised that the organ culture system lacks an inflammatory system (similar to an intact IVD); therefore, the exclusion of surrounding tissues removes any potential immune infiltration or systemic effect. The *ex vivo* model presented would be best utilised in the short-term to rapidly screen the initial effects of potential treatments, before performing long-term studies to determine full repair in living animal systems that aim to ensure safety matters prior to clinical trials.

As *ex vivo* studies in bioreactors are limited to 3-4 weeks for practical reasons, the main challenge of the study was to induce a fast and reproducible IVD degeneration, to allow a sufficient time for the regenerative treatment to show its efficacy. To assure reproducibility, healthy IVDs were taken from not too old adult goats (3-5 years). Such healthy discs have similar characteristics and serve well as a reference, both for degeneration and regeneration studies. A complicating factor for creating a degeneration model is that the cause of disc degeneration in humans is generally unknown (Urban and Roberts, 2003). Indeed, various mechanisms have been described, varying from genetic to purely mechanical (Kandel *et al.*, 2008; Schnake *et al.*, 2006; Urban and Roberts, 2003), although the presence of a catabolic phenotype is well characterised within human disc degeneration (Table1) and, thus, can be a useful cellular process to mimic in an *ex vivo* model. This implies that a disc degeneration model may look like human disc degeneration but does not necessarily represent the physiological induction of degeneration of specific patients. Furthermore, human discs generally degenerate over a relatively long period of time. This implies that induction of disc degeneration must not only be directed to mechanics and cells but also to the extracellular matrix, which is inherently related to mechanical behaviour and cell properties (Vergroesen *et al.*, 2015).

The mechanism of degeneration by cABC is attributed to the degeneration of the chondroitin sulphate chains of proteoglycans, whereas collagenase induces disc degradation by breaking the peptide bonds in collagen (Eckhard *et al.*, 2014; Prabhakar *et al.*, 2005). Thus, the combined effects modulate the key matrix components of the NP (*i.e.* proteoglycans and collagens). There are several other studies that have used cABC or collagenase as inducers of IVD degradation *in vivo*. For example, Ghosh *et al.* (2012) have injected cABC intradiscally in the lumbar discs of male adult sheep and have observed a decrease in disc height of 45-50 % after 3 months *in vivo*. Sasaki *et al.* (2001) have used relatively high doses of cABC (*i.e.* up to 50 U) and have demonstrated a decrease in ovine IVD height of 15 % after 1 week and 30 % after 4 weeks. In a rhesus monkey model, Stern and Coulson (1976) have identified a loss of disc height 7 d after collagenase injection. The same findings were observed by Growney Kalaf *et al.* (2014), who have shown decreased disc height 48 h after injecting collagenase into young bovine IVDs. Hoogendoorn *et al.* (2007) have found disc degeneration without signs of severe degeneration after injection of 0.25 U/mL cABC at 12 weeks. The same effect was shown by Gullbrand *et al.* (2017), who have demonstrated that the injection of cABC and nucleotomy cause moderate disc degeneration in goats, with a follow-up after injection of 12 weeks. A follow-up study by Zhang *et al.* (2020) has recently demonstrated that this model induces also a catabolic phenotype similar to that observed in the present study. In a study involving the same bioreactor as the one used in the present study as well as using cABC to induce IVD degeneration (Paul *et al.*, 2018), disc degeneration was identified graded on the Pfirrmann scale as 2-4. However, this induction was only following 20 d of culture and, thus, not suitable for application of regenerative therapy investigation. Furthermore,

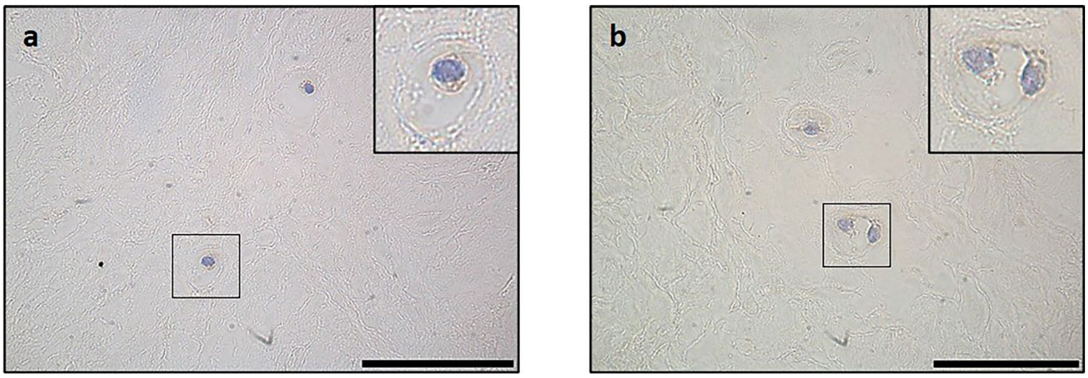

Fig. 7. Negative control IHC staining of caprine IVD tissue. (**a**) Mouse monoclonal IgG1, kappa) isotype control staining. (**b**) Rabbit polyclonal IgG isotype control staining. IgG controls were used at the same protein concentration as primary antibodies. Inlets show magnified images demonstrating clear negative IHC for isotype controls on caprine IVD tissue. Cell nuclei counterstained with Mayer's haematoxylin. Scale bar: 50 μm.

Paul *et al.* (2018) have not determined whether a true catabolic phenotype was induced. Therefore, the current study utilised a slightly higher dose of cABC combined with collagenase to induce a more rapid degenerative effect, whilst also decreasing both proteoglycans and collagens within the disc, and determine the cellular phenotype following load. The study demonstrated the induction of moderate degeneration with cellular changes akin to those seen during human disc degeneration (Boos *et al.*, 2002; Gries *et al.*, 2000; Rutges *et al.*, 2013; Sive *et al.*, 2002). Importantly, the induced changes in cellular phenotype with increased expression of the catabolic cytokine IL-1 and its downstream targets, such as MMPs, ADAMTS and other catabolic cytokines, nerve inducers and angiogenic factors provided a model in which not only effects on matrix synthesis and biomechanical factors could be determined. This provided a potential model that mimicked more closely the degradative cascade seen during human disc degeneration (Binch *et al.*, 2014; Le Maitre *et al.*, 2005; Le Maitre *et al.*, 2015; Phillips *et al.*, 2015; Risbud and Shapiro, 2014; Vo *et al.*, 2016) and, thus, could be utilised to investigate therapies targeting the cellular changes seen during disc degeneration as well as supporting tissue regeneration.

The current study had several limitations. Firstly, loading was restricted to 7 d post-enzyme injection, which followed 3 d of preload. This time course may be too short to develop a new equilibrium after inducing degeneration, which was suggested from the continual decline in creep behaviour. However, IDD is a dynamic process of matrix degradation and altered biomechanical behaviour (Vergroesen *et al.*, 2015) and the biomechanical response of cABC- and collagenase-degenerated discs might reflect this. This was supported by the increased expression of matrix-degrading enzymes, suggesting that natural degeneration was ongoing and, thus, an equilibrium might not be possible, as may be the case for human disc degeneration. Also, the study did not investigate the injection of collagenase or chondroitinase alone within the LDCS; however, single injections were investigated in preliminary studies to determine enzyme concentrations for further investigation. The combination of both enzymes demonstrated disruption of both collagens and proteoglycans, mimicking more closely what seen during early human disc degeneration and, thus, were selected for investigation within the LDCS. Whilst the objective of producing a rapid, reproducible *ex vivo* model of IVD degeneration was still achieved, any specific effect of each enzyme or dose response cannot be inferred within the LDCS. Secondly, an increase in time constants for the enzyme-degenerated discs was seen, while there were decreases in time constants for the control group. However, this was not significant and might be explained by the small sample size of the control group.

This caprine model for moderate IVD degeneration, which combined the use of cABC and collagenase to induce a rapid onset of degeneration that simulated human disc degeneration, provided a good base for further research, suggesting its suitability as an *ex vivo* model for regenerative therapeutics that aim to interfere with the vicious cycle of disc degeneration (Thorpe *et al.*, 2018; Vergroesen *et al.*, 2015).

Conclusion

The study of restorative therapeutics for IVD degeneration is hindered by the lack of fast, reproducible *ex vivo* models that closely represent human IVD degeneration, prior to the use of expensive, time-consuming animal models. The present study established a fast and reproducible, large-animal *ex vivo* model of disc degeneration. This model system has the potential for use in the rapid screening of novel restorative therapeutics, such as biologics, biomaterials and cell therapies, enabling short-term predictors of repair that may reduce the dependence on animal studies.

Acknowledgements

The authors would like to thank Versus Arthritis and the MRC (MR/P026796/1) for funding.

References

Adams MA, Roughley PJ (2006) What is intervertebral disc degeneration, and what causes it? Spine (Phila Pa 1976) **31**: 2151-2161.

Alini M, Eisenstein SM, Ito K, Little C, Kettler AA, Masuda K, Melrose J, Ralphs J, Stokes I, Wilke HJ (2008) Are animal models useful for studying human disc disorders/degeneration? Eur Spine J **17**: 2-19.

Anderson DG, Risbud M V, Shapiro IM, Vaccaro AR, Albert TJ (2005) Cell-based therapy for disc repair. Spine J **5**: 297S-303S.

Binch A, Cole AA, Breakwell LM, Michael AL, Chiverton N, Cross AK, Le Maitre CL (2014) Expression and regulation of neurotrophic and angiogenic factors during human intervertebral disc degeneration. Arthritis Res Ther **16**: 416. DOI: 10.1186/s13075-014-0416-1.

Binch ALA, Cole AA, Breakwell LM, Michael ALR, Chiverton N, Creemers LB, Cross AK, Le Maitre CL (2015) Nerves are more abundant than blood vessels in the degenerate human intervertebral disc. Arthritis Res Ther **17**. DOI: 10.1186/s13075-015-0889-6.

Boos N, Weissbach S, Rohrbach H, Weiler C, Spratt KF, Nerlich AG (2002) Classification of age-related changes in lumbar intervertebral discs: 2002 Volvo award in basic science. Spine (Phila Pa 1976) **27**: 2631-2644.

Daly C, Ghosh P, Jenkin G, Oehme D, Goldschlager T (2016) A review of animal models of intervertebral disc degeneration: pathophysiology, regeneration, and translation to the clinic. Biomed Res Int: 5952165. DOI: 10.1155/2016/5952165.

de Schepper EIT, Damen J, van Meurs JBJ, Ginai AZ, Popham M, Hofman A, Koes BW, Bierma-Zeinstra SM (2010) The association between lumbar disc degeneration and low back pain: the influence of age, gender, and individual radiographic features. Spine (Phila Pa 1976) **35**: 531-536.

Doita M, Kanatani T, Harada T, Mizuno K (1996) Immunohistologic study of the ruptured intervertebral disc of the lumbar spine. Spine (Phila Pa 1976) **21**: 235-241.

Eckhard U, Huesgen PF, Brandstetter H, Overall CM (2014) Proteomic protease specificity profiling of clostridial collagenases reveals their intrinsic nature as dedicated degraders of collagen. J Proteomics **100**: 102-114.

Emanuel KS, Vergroesen P-PA, Peeters M, Holewijn RM, Kingma I, Smit TH (2015) Poroelastic behaviour of the degenerating human intervertebral disc: a ten-day study in a loaded disc culture system. Eur Cells Mater **29**: 330-341.

Gantenbein B, Illien-Jünger S, Chan S, Walser J, Haglund L, Ferguson S, Iatridis J, Grad S (2015) Organ culture bioreactors - platforms to study human intervertebral disc degeneration and regenerative therapy. Curr Stem Cell Res Ther **10**: 339-352.

Ghosh P, Moore R, Vernon-Roberts B, Goldschlager T, Pascoe D, Zannettino A, Gronthos S, Itescu S (2012) Immunoselected STRO-3 $^+$ mesenchymal precursor cells and restoration of the extracellular matrix of degenerate intervertebral discs. J Neurosurg Spine **16**: 479-488.

Gries NC, Berlemann U, Moore RJ, Vernon-Roberts B (2000) Early histologic changes in lower lumbar discs and facet joints and their correlation. Eur Spine J **9**: 23-29.

Growney Kalaf EA, Sell SA, Bledsoe JG (2014) Developing a mechanical and chemical model of degeneration in young bovine lumbar intervertebral disks and reversing loss in mechanical function. J Spinal Disord Tech **27**: E168-175.

Gullbrand SE, Malhotra NR, Schaer TP, Zawacki Z, Martin JT, Bendigo JR, Milby AH, Dodge GR, Vresilovic EJ, Elliott DM, Mauck RL, Smith LJ (2017) A large animal model that recapitulates the spectrum of human intervertebral disc degeneration. Osteoarthr Cartil **25**: 146-156.

Hoogendoorn RJ (2009) Studies on the degeneration and regeneration of the intervertebral disc. VU University Medical Center.

Hoogendoorn R, Wuisman P, Smit T, Everts V, Helder M (2007) Experimental intervertebral disc degeneration induced by chondroitinase ABC in the goat. Spine (Phila Pa 1976) **32**: 1816-1825.

Hoyland JA, Le Maitre C, Freemont AJ (2008) Investigation of the role of IL-1 and TNF in matrix degradation in the intervertebral disc. Rheumatology **47**: 809-814.

Iatridis JC, Setton LA, Weidenbaum M, Mow VC (1997) Alterations in the mechanical behavior of the human lumbar nucleus pulposus with degeneration and aging. J Orthop Res **15**: 318-322.

Iatridis JC, Kumar S, Foster RJ, Weidenbaum M, Mow VC (1999) Shear mechanical properties of human lumbar annulus fibrosus. J Orthop Res **17**: 732-737.

Kandel R, Roberts S, Urban JP (2008) Tissue engineering and the intervertebral disc: the challenges. Eur Spine J **17** Suppl 4: 480-491.

Korecki CL, MacLean JJ, Iatridis JC (2008) Dynamic compression effects on intervertebral disc mechanics and biology. Spine (Phila Pa 1976) **33**: 1403-1409.

Krijnen M, Mensch D, Van Dieen J, Wuisman P, Smit T (2006) Primary spinal segment stability with a stand-alone cage: *in vitro* evaluation of a successful goat model. Acta Orthop **77**: 454-461.

Lama P, Le Maitre CL, Harding IJ, Dolan P, Adams MA (2018) Nerves and blood vessels in degenerated intervertebral discs are confined to physically disrupted tissue. J Anat **233**: 86-97.

Lang G, Liu Y, Geries J, Zhou Z, Kubosch D, Südkamp N, Richards RG, Alini M, Grad S, Li Z (2018) An intervertebral disc whole organ culture system to investigate proinflammatory and degenerative disc disease condition. J Tissue Eng Regen Med **12**: e2051-e2061.

Le Maitre CL, Freemont AJ, Hoyland JA (2004) Localization of degradative enzymes and their inhibitors in the degenerate human intervertebral disc. J Pathol **204**: 47-54.

Le Maitre, Binch, Thorpe, Hughes (2015) Degeneration of the intervertebral disc with new approaches for treating low back pain. J Neurosurg Sci **59**: 47-61.

Le Maitre, Freemont, Hoyland (2005) The role of interleukin-1 in the pathogenesis of human intervertebral disc degeneration. Arthritis Res Ther **7**: R732-475.

Le Maitre, Pockert, Buttle, Freemont, Hoyland (2007) Matrix synthesis and degradation in human intervertebral disc degeneration. Biochem Soc Trans **35**: 652-655.

McMillan DW, Garbutt G, Adams MA (1996) Effect of sustained loading on the water content of intervertebral discs: implications for disc metabolism. Ann Rheum Dis **55**: 880-887.

Ohshima H, Tsuji H HN (1989) Water diffusion pathway,swelling pressure, and biomechanical properties of the intervertebral disc during compression load. Spine (Phila Pa 1976) **14**: 1234-1244.

Paul CPL, Smit TH, de Graaf M, Holewijn RM, Bisschop A, van de Ven PM, Mullender MG, Helder MN, Strijkers GJ (2018) Quantitative MRI in early intervertebral disc degeneration: T1rho correlates better than T2 and ADC with biomechanics, histology and matrix content. PLoS One **13**: e0191442. DOI: 10.1371/journal.pone.0191442.

Paul CPL, Schoorl T, Zuiderbaan HA, Zandieh Doulabi B, van der Veen AJ, van de Ven PM, Smit TH, van Royen BJ, Helder MN, Mullender MG

(2013) Dynamic and static overloading induce early degenerative processes in caprine lumbar intervertebral discs. PLoS One **8**: e62411. DOI: 10.1371/journal.pone.0062411.

Paul CPL, Zuiderbaan HA, Doulabi BZ, Van Der Veen AJ, Van De Ven PM, Smit TH, Helder MN, Van Royen BJ, Mullender MG (2012) Simulated-physiological loading conditions preserve biological and mechanical properties of caprine lumbar intervertebral discs in *ex vivo* culture. PLoS One **7**. DOI: 10.1371/journal.pone.0033147.

Pfannkuche J-J, Guo W, Cui S, Ma J, Lang G, Peroglio M, Richards RG, Alini M, Grad S, Li Z (2019) Intervertebral disc organ culture for the investigation of disc pathology and regeneration – benefits, limitations, and future directions of bioreactors. Connect Tissue Res: **61**: 304-321.

Pfirrmann CWA, Metzdorf A, Zanetti M, Hodler J, Boos N (2001) Magnetic resonance classification of lumbar intervertebral disc degeneration. Spine (Phila Pa 1976) **26**: 1873-1878.

Phillips KLE, Cullen K, Chiverton N, Michael ALR, Cole AA, Breakwell LM, Haddock G, Bunning RAD, Cross AK, Le Maitre CL (2015) Potential roles of cytokines and chemokines in human intervertebral disc degeneration: interleukin-1 is a master regulator of catabolic processes. Osteoarthr Cartil **23**: 1165-1177.

Phillips KLE, Chiverton N, Michael ALR, Cole AA, Breakwell LM, Haddock G, Bunning RAD, Cross AK, Le Maitre CL (2013) The cytokine and chemokine expression profile of nucleus pulposus cells: Implications for degeneration and regeneration of the intervertebral disc. Arthritis Res Ther **15**: R213. DOI: 10.1186/ar4408.

Pockert AJ, Richardson SM, Le Maitre CL, Lyon M, Deakin JA, Buttle DJ, Freemont AJ, Hoyland JA (2009) Modified expression of the ADAMTS enzymes and tissue inhibitor of metalloproteinases 3 during human intervertebral disc degeneration. Arthritis Rheum **60**: 482-491.

Prabhakar V, Capila I, Bosques CJ, Pojasek K, Sasisekharan R (2005) Chondroitinase ABC I from *Proteus vulgaris*: cloning, recombinant expression and active site identification. Biochem J **386**: 103-112.

Pye SR, Reid DM, Smith R, Adams JE, Nelson K, Silman AJ, O'Neill TW (2004) Radiographic features of lumbar disc degeneration and self-reported back pain. J Rheumatol **31**: 753-758.

Rätsep T, Minajeva A, Asser T (2013) Relationship between neovascularization and degenerative changes in herniated lumbar intervertebral discs. Eur Spine J **22**: 2474-2480. DOI: 10.1007/s00586-013-2842-1.

Risbud M V., Shapiro IM (2014) Role of cytokines in intervertebral disc degeneration: pain and disc content. Nat Rev Rheumatol **10**: 44-56.

Roberts S, Hollander AP, Caterson B, Menage J, Richardson JB (2001) Matrix turnover in human cartilage repair tissue in autologous chondrocyte implantation. Arthritis Rheum **44**: 2586-2598.

Roberts S, Menage J, Duance V, Wotton S, Ayad S (1991) 1991 Volvo Award in basic sciences. Collagen types around the cells of the intervertebral disc and cartilage end plate: an immunolocalization study. Spine (Phila Pa 1976) **16**: 1030-1038.

Roberts S, Menage J, Sivan S, Urban JPG (2008) Bovine explant model of degeneration of the intervertebral disc. BMC Musculoskelet Disord **9**: 24. DOI: 10.1186/1471-2474-9-24.

Rosenzweig DH, Gawri R, Moir J, Beckman L, Eglin D, Steffen T, Roughley PJ, Ouellet JA, Haglund L (2016) Dynamic loading, matrix maintenance and cell injection therapy of human intervertebral discs cultured in a bioreactor. Eur Cells Mater **31**: 26-39.

Roughley PJ (2004) Biology of intervertebral disc aging and degeneration: involvement of the extracellular matrix. Spine (Phila Pa 1976) **29**: 2691-2699.

Rutges JPHJ, Duit RA, Kummer JA, Bekkers JEJ, Oner FC, Castelein RM, Dhert WJA, Creemers LB (2013) A validated new histological classification for intervertebral disc degeneration. Osteoarthr Cartil **21**: 2039-2047.

Sasaki M, Takahashi T, Miyahara K, Hirose T (2001) Effects of chondroitinase ABC on intradiscal pressure in sheep: an *in vivo* study. Spine (Phila Pa 1976) **26**: 463-468.

Schnake KJ, Putzier M, Haas NP, Kandziora F (2006) Mechanical concepts for disc regeneration. Eur Spine J **15** Suppl 3: S354-S360.

Schutgens EM (2015) Biomaterials for intervertebral disc regeneration: past performance and possible future strategies. Eur Cell Mater **30**: 210-231.

Séguin CA, Bojarski M, Pilliar RM, Roughley PJ, Kandel RA (2006) Differential regulation of matrix degrading enzymes in a TNFalpha-induced model of nucleus pulposus tissue degeneration. Matrix Biol **25**: 409-418.

Shapiro IM, Vresilovic EJ, Risbud MV (2012) Is the spinal motion segment a diarthrodial polyaxial joint: what is a nice nucleus like you doing in a joint like this? Bone **50**: 771-776.

Sive JI, Baird P, Jeziorsk M, Watkins A, Hoyland JA, Freemont AJ (2002) Expression of chondrocyte markers by cells of normal and degenerate intervertebral discs. Mol Pathol **55**: 91-97.

Smit TH (2002) The use of a quadruped as an *in vivo* model for the study of the spine – biomechanical considerations. Eur Spine J **11**: 137-144.

Stern WE, Coulson WF (1976) Effects of collagenase upon the intervertebral disc in monkeys. J Neurosurg **44**: 32-44.

Sun Z, Liu B, Luo ZJ (2020) The immune privilege of the intervertebral disc: implications for intervertebral disc degeneration treatment. Int J Med Sci **17**: 685-692.

Teixeira GQ, Boldt A, Nagl I, Pereira CL, Benz K, Wilke H-J, Ignatius A, Barbosa MA, Goncalves RM, Neidlinger-Wilke C (2015) A degenerative/ proinflammatory intervertebral disc organ culture:

an *ex vivo* model for anti-inflammatory drug and cell therapy. Tissue Eng Part C Methods **22**: 1-12.

Thorpe AA, Dougill G, Vickers L, Reeves ND, Sammon C, Cooper G, Le Maitre CL (2017) Thermally triggered hydrogel injection into bovine intervertebral disc tissue explants induces differentiation of mesenchymal stem cells and restores mechanical function. Acta Biomater **54**: 212-226.

Thorpe AA, Boyes VL, Sammon C, Le Maitre CL (2016) Thermally triggered injectable hydrogel, which induces mesenchymal stem cell differentiation to nucleus pulposus cells: potential for regeneration of the intervertebral disc. Acta Biomater **36**: 99-111.

Thorpe AA, Bach FC, Tryfonidou MA, Le Maitre CL, Mwale F, Diwan AD, Ito K (2018) Leaping the hurdles in developing regenerative treatments for the intervertebral disc from preclinical to clinical. JOR Spine **1**: e1027. DOI: 10.1002/jsp2.1027.

Tsujimoto T, Sudo H, Todoh M, Yamada K, Iwasaki K, Ohnishi T, Hirohama N, Nonoyama T, Ukeba D, Ura K, Ito YM, Iwasaki N (2018) An acellular bioresorbable ultra-puri fi ed alginate gel promotes intervertebral disc repair: a preclinical proof-of-concept study. EBioMedicine **37**: 17-21.

van Tulder MW, Assendelft WJ, Koes BW, Bouter LM (1997) Spinal radiographic findings and nonspecific low back pain. A systematic review of observational studies. Spine (Phila Pa 1976) **2**: 427-34.

Urban JPG, Roberts S (2003) Degeneration of the intervertebral disc. Arthritis Res Ther **5**: 120-130.

van der Veen AJ, van Dieën JH, Nadort A, Stam B, Smit TH (2007) Intervertebral disc recovery after dynamic or static loading *in vitro*: Is there a role for the endplate? J Biomech **40**: 2230-2235.

Vergroesen P-PA, Kingma I, Emanuel KS, Hoogendoorn RJ, Welting TJ, van Royen BJ, van Dieën JH, Smit TH (2015) Mechanics and biology in intervertebral disc degeneration: a vicious circle. Osteoarthr Cartil **23**: 1057-1070.

Vo N V, Hartman RA, Patil PR, Risbud M V, Kletsas D, Iatridis JC, Hoyland JA, Le Maitre CL, Sowa GA, Kang JD (2016) Molecular mechanisms of biological aging in intervertebral discs. J Orthop Res **34**: 1289-306.

Vos T, Abajobir AA, Abbafati C, Abbas KM, Abate KH, Abd-Allah F, Abdulle AM, Abebo TA, Abera SF, Aboyans V, Abu-Raddad LJ, Ackerman IN, Adamu AA, Adetokunboh O, Afarideh M, Afshin A, Agarwal SK, Aggarwal R, Agrawal A, Agrawal S, Ahmad Kiadaliri A, Ahmadieh H, Ahmed MB, Aichour AN, Aichour I, Aichour MTE, Aiyar S, Akinyemi RO, Akseer N, Al Lami FH, Alahdab F, Al-Aly Z, Alam K, Alam N, Alam T, Alasfoor D, Alene KA, Ali R, Alizadeh-Navaei R, Alkerwi A, Alla F, Allebeck P, Allen C, Al-Maskari F, Al-Raddadi R, Alsharif U, Alsowaidi S, Altirkawi KA, Amare AT, Amini E, Ammar W, Amoako YA, Andersen HH, Antonio CAT, Anwari P, Ärnlöv J, Artaman A, Aryal KK, Asayesh H, Asgedom SW, Assadi R, Atey TM, Atnafu NT, Atre SR, Avila-Burgos L, Avokpaho EFGA, Awasthi A, Ayala Quintanilla BP, Ba Saleem HO, Bacha U, Badawi A, Balakrishnan K, Banerjee A, Bannick MS, Barac A, Barber RM, Barker-Collo SL, Bärnighausen T, Barquera S, Barregard L, Barrero LH, Basu S, Battista B, Battle KE, Baune BT, Bazargan-Hejazi S, Beardsley J, Bedi N, Beghi E, Béjot Y, Bekele BB, Bell ML, Bennett DA, Bensenor IM, Benson J, Berhane A, Berhe DF, Bernabé E, Betsu BD, Beuran M, Beyene AS, Bhala N, Bhansali A, Bhatt S, Bhutta ZA, Biadgilign S, Bienhoff K, Bikbov B, Birungi C, Biryukov S, Bisanzio D, Bizuayehu HM, Boneya DJ, Boufous S, Bourne RRA, Brazinova A, Brugha TS, Buchbinder R, Bulto LNB, Bumgarner BR, Butt ZA, Cahuana-Hurtado L, Cameron E, Car M, Carabin H, Carapetis JR, Cárdenas R, Carpenter DO, Carrero JJ, Carter A, Carvalho F, Casey DC, Caso V, Castañeda-Orjuela CA, Castle CD, Catalá-López F, Chang HY, Chang JC, Charlson FJ, Chen H, Chibalabala M, Chibueze CE, Chisumpa VH, Chitheer AA, Christopher DJ, Ciobanu LG, Cirillo M, Colombara D, Cooper C, Cortesi PA, Criqui MH, Crump JA, Dadi AF, Dalal K, Dandona L, Dandona R, Das Neves J, Davitoiu D V., De Courten B, De Leo D, Degenhardt L, Deiparine S, Dellavalle RP, Deribe K, Des Jarlais DC, Dey S, Dharmaratne SD, Dhillon PK, Dicker D, Ding EL, Djalalinia S, Do HP, Dorsey ER, Dos Santos KPB, Douwes-Schultz D, Doyle KE, Driscoll TR, Dubey M, Duncan BB, El-Khatib ZZ, Ellerstrand J, Enayati A, Endries AY, Ermakov SP, Erskine HE, Eshrati B, Eskandarieh S, Esteghamati A, Estep K, Fanuel FBB, Farinha CSES, Faro A, Farzadfar F, Fazeli MS, Feigin VL, Fereshtehnejad SM, Fernandes JC, Ferrari AJ, Feyissa TR, Filip I, Fischer F, Fitzmaurice C, Flaxman AD, Flor LS, Foigt N, Foreman KJ, Franklin RC, Fullman N, Fürst T, Furtado JM, Futran ND, Gakidou E, Ganji M, Garcia-Basteiro AL, Gebre T, Gebrehiwot TT, Geleto A, Gemechu BL, Gesesew HA, Gething PW, Ghajar A, Gibney KB, Gill PS, Gillum RF, Ginawi IAM, Giref AZ, Gishu MD, Giussani G, Godwin WW, Gold AL, Goldberg EM, Gona PN, Goodridge A, Gopalani SV, Goto A, Goulart AC, Griswold M, Gugnani HC, Gupta R, Gupta R, Gupta T, Gupta V, Hafezi-Nejad N, Hailu AD, Hailu GB, Hamadeh RR, Hamidi S, Handal AJ, Hankey GJ, Hao Y, Harb HL, Hareri HA, Haro JM, Harvey J, Hassanvand MS, Havmoeller R, Hawley C, Hay RJ, Hay SI, Henry NJ, Heredia-Pi IB, Heydarpour P, Hoek HW, Hoffman HJ, Horita N, Hosgood HD, Hostiuc S, Hotez PJ, Hoy DG, Htet AS, Hu G, Huang H, Huynh C, Iburg KM, Igumbor EU, Ikeda C, Irvine CMS, Jacobsen KH, Jahanmehr N, Jakovljevic MB, Jassal SK, Javanbakht M, Jayaraman SP, Jeemon P, Jensen PN, Jha V, Jiang G, John D, Johnson CO, Johnson SC, Jonas JB, Jürisson M, Kabir Z, Kadel R, Kahsay A, Kamal R, Kan H, Karam NE, Karch A, Karema CK, Kasaeian A, Kassa GM, Kassaw NA, Kassebaum NJ, Kastor A, Katikireddi SV, Kaul A, Kawakami N, Keiyoro PN, Kengne AP, Keren A, Khader YS, Khalil IA, Khan EA, Khang YH, Khosravi A, Khubchandani J, Kieling C, Kim D, Kim P, Kim YJ, Kimokoti RW, Kinfu Y, Kisa A, Kissimova-Skarbek KA, Kivimaki M, Knudsen AK, Kokubo Y, Kolte D, Kopec JA, Kosen S, Koul PA, Koyanagi A, Kravchenko M, Krishnaswami S, Krohn KJ, Kuate Defo B, Kucuk Bicer B, Kumar GA, Kumar P, Kumar S, Kyu HH, Lal DK, Lalloo R, Lambert N, Lan Q, Larsson A, Lavados PM, Leasher JL, Lee JT, Lee PH, Leigh J, Leshargie CT, Leung J, Leung R, Levi M, Li Y, Li Y, Li Kappe D, Liang X, Liben ML, Lim SS, Linn S, Liu A, Liu PY, Liu S, Liu Y, Lodha R, Logroscino G, London SJ, Looker KJ, Lopez AD, Lorkowski S, Lotufo PA, Low N, Lozano R, Lucas TCD, Macarayan ERK, Magdy Abd El Razek H, Magdy Abd El Razek M, Mahdavi M, Majdan M, Majdzadeh R, Majeed A, Malekzadeh R, Malhotra R, Malta DC, Mamun AA, Manguerra H, Manhertz T, Mantilla A, Mantovani LG, Mapoma CC, Marczak LB, Martinez-Raga J, Martins-Melo FR, Martopullo I, März W, Mathur MR, Mazidi M, McAlinden C, McGaughey M, McGrath JJ, McKee M, McNellan C, Mehata S, Mehndiratta MM, Mekonnen TC, Memiah P, Memish ZA, Mendoza W, Mengistie MA, Mengistu DT, Mensah GA, Meretoja A, Meretoja TJ, Mezgebe HB, Micha R, Millear A, Miller TR, Mills EJ, Mirarefin M, Mirrakhimov EM, Misganaw A, Mishra SR, Mitchell PB, Mohammad KA, Mohammadi A, Mohammed KE, Mohammed S, Mohanty SK, Mokdad AH, Mollenkopf SK, Monasta L, Hernandez JM, Montico M, Moradi-Lakeh M, Moraga P, Mori R, Morozoff C, Morrison SD, Moses M, Mountjoy-Venning C, Mruts KB, Mueller UO, Muller K, Murdoch ME, Murthy GVS, Musa KI, Nachega JB, Nagel G, Naghavi M, Naheed A, Naidoo KS, Naldi L, Nangia V, Natarajan G, Negasa DE, Negoi I, Negoi RI, Newton CR, Ngunjiri JW, Nguyen CT, Nguyen G, Nguyen M, Nguyen Q Le, Nguyen TH, Nichols E, Ningrum DNA, Nolte S, Nong VM, Norrving B, Noubiap JJN, O'Donnell MJ, Ogbo FA, Oh IH, Okoro A, Oladimeji O, Olagunju AT, Olagunju TO, Olsen HE, Olusanya BO, Olusanya JO, Ong K, Opio JN, Oren E, Ortiz A, Osgood-Zimmerman A, Osman M, Owolabi MO, Pa M, Pacella RE, Pana A, Panda BK, Papachristou C, Park EK, Parry CD, Parsaeian M, Patten SB, Patton GC, Paulson K, Pearce N, Pereira DM, Perico N, Pesudovs K, Peterson CB, Petzold M, Phillips MR, Pigott DM, Pillay JD, Pinho C, Plass D, Pletcher MA, Popova S, Poulton RG, Pourmalek F, Prabhakaran D, Prasad N, Prasad NM, Purcell C, Qorbani M, Quansah R, Rabiee RHS, Radfar A, Rafay A, Rahimi K, Rahimi-Movaghar A, Rahimi-Movaghar V, Rahman M, Rahman MHU, Rai RK, Rajsic S, Ram U, Ranabhat CL, Rankin Z, Rao PV, Rao PC, Rawaf S, Ray SE, Reiner RC, Reinig N, Reitsma MB, Remuzzi G, Renzaho AMN, Resnikoff S, Rezaei S, Ribeiro AL, Ronfani L, Roshandel G, Roth GA, Roy A, Rubagotti E, Ruhago GM, Saadat S, Sadat N, Safdarian M, Safi S, Safiri S, Sagar R, Sahathevan R, Salama J, Salomon JA, Salvi SS, Samy AM, Sanabria JR, Santomauro D, Santos IS, Santos JV, Santric Milicevic MM, Sartorius B, Satpathy M, Sawhney M, Saxena S, Schmidt MI, Schneider IJC, Schöttker B, Schwebel DC, Schwendicke F, Seedat S, Sepanlou SG, Servan-Mori EE, Setegn T, Shackelford KA, Shaheen A, Shaikh MA, Shamsipour M, Shariful Islam SM, Sharma J, Sharma R, She J, Shi P, Shields C, Shigematsu M, Shinohara Y, Shiri R, Shirkoohi R, Shirude S, Shishani K, Shrime MG, Sibai AM, Sigfusdottir ID, Silva DAS, Silva JP, Silveira DGA, Singh JA, Singh NP, Sinha DN, Skiadaresi E, Skirbekk V, Slepak EL, Sligar A, Smith DL, Smith M, Sobaih BHA, Sobngwi E, Sorensen RJD, Sousa TCM, Sposato LA, Sreeramareddy CT, Srinivasan V, Stanaway JD, Stathopoulou V, Steel N, Stein DJ, Stein MB, Steiner C, Steiner TJ, Steinke S, Stokes MA, Stovner LJ, Strub B, Subart M, Sufiyan MB, Suliankatchi Abdulkader R, Sunguya BF, Sur PJ, Swaminathan S, Sykes BL, Sylte DO, Tabarés-Seisdedos R, Taffere GR, Takala JS, Tandon N, Tavakkoli M, Taveira N, Taylor HR, Tehrani-Banihashemi A, Tekelab T, Temam Shifa G, Terkawi AS, Tesfaye DJ, Tesssema B, Thamsuwan O, Thomas KE, Thrift AG, Tiruye TY, Tobe-Gai R, Tollanes MC, Tonelli M, Topor-Madry R, Tortajada M, Touvier M, Tran BX, Tripathi S, Troeger C, Truelsen T, Tsoi D, Tuem KB, Tuzcu EM, Tyrovolas S, Ukwaja KN, Undurraga EA, Uneke CJ, Updike R, Uthman OA, Uzochukwu BSC, Van Boven JFM, Varughese S, Vasankari T, Venkatesh S, Venketasubramanian N, Vidavalur R, Violante FS, Vladimirov SK, Vlassov VV, Vollset SE, Wadilo F, Wakayo T, Wang YP, Weaver M, Weichenthal S, Weiderpass E, Weintraub RG, Werdecker A, Westerman R, Whiteford HA, Wijeratne T, Wiysonge CS, Wolfe CDA, Woodbrook R, Woolf AD, Workicho A, Wulf Hanson S, Xavier D, Xu G, Yadgir S, Yaghoubi M, Yakob B, Yan LL, Yano Y, Ye P, Yimam HH, Yip P, Yonemoto N, Yoon SJ, Yotebieng M, Younis MZ, Zaidi Z, Zaki MES, Zegeye EA, Zenebe ZM, Zhang X, Zhou M, Zipkin B, Zodpey S, Zuhlke LJ, Murray CJL (2017) Global, regional, and national incidence, prevalence, and years lived with disability for 328 diseases and injuries for 195 countries, 1990-2016: a systematic analysis for the Global Burden of Disease Study 2016. Lancet **390**: 1211-1259.

Walter BA, Illien-Jünger S, Nasser PR, Hecht AC, Iatridis JC (2014) Development and validation of a bioreactor system for dynamic loading and mechanical characterization of whole human intervertebral discs in organ culture. J Biomech **47**: 2095-2101.

Walter BA, Korecki CL, Purmessur D, Roughley PJ, Michalek AJ, Iatridis JC (2011) Complex loading affects intervertebral disc mechanics and biology. Osteoarthr Cartil **19**: 1011-1018.

Walter BA, Likhitpanichkul M, Illien-Junger S, Roughley PJ, Hecht AC, Iatridis JC (2015) TNFα transport induced by dynamic loading alters biomechanics of intact intervertebral discs. PLoS One **10**: e0118358. DOI: 10.1371/journal.pone.0118358.

Wang D-L, Jiang S-D, Dai L-Y (2007) Biologic response of the intervertebral disc to static and dynamic compression *in vitro*. Spine (Phila Pa 1976) **32**: 2521-2528.

Weber KT, Jacobsen TD, Maidhof R, Virojanapa J, Overby C, Bloom O, Quraishi S, Levine M, Chahine NO (2015) Developments in intervertebral disc disease research: pathophysiology, mechanobiology, and therapeutics. Curr Rev Musculoskelet Med **8**: 18-31.

Wei F, Zhong R, Zhou Z, Wang L, Pan X, Cui S, Zou X, Gao M, Sun H, Chen W, Liu S (2014) In vivo experimental intervertebral disc degeneration induced by bleomycin in the rhesus monkey. BMC Musculoskelet Disord **15**: 340. DOI: 10.1186/1471-2474-15-340.

Wuertz K, Godburn K, MacLean JJ, Barbir A, Stinnett Donnelly J, Roughley PJ, Alini M, Iatridis JC (2009) In vivo remodeling of intervertebral discs in response to short- and long-term dynamic compression. J Orthop Res **27**: 1235-1242.

Yajun W, Yue Z, Xiuxin H, Cui C (2010) A meta-analysis of artificial total disc replacement *versus* fusion for lumbar degenerative disc disease. Eur Spine J **19**: 1250-1261.

Zhang C, Gullbrand SE, Schaer TP, Lau YK, Jiang Z, Dodge GR, Elliott DM, Mauck RL, Malhotra NR, Smith LJ (2020) Inflammatory cytokine and catabolic enzyme expression in a goat model of intervertebral disc degeneration. J Orthop Res. DOI: 10.1002/jor.24639.

Discussion with Reviewers

Reviewer 1: Do the authors believe this model system would reduce or fully eliminate the use of live animal testing?

Authors: We feel that this model will be particularly useful in enabling the screening of potential new therapies under loading environments more closely matching clinical applications. This will enable only the most promising therapies to be selected to go forwards for animal testing as a pre-requisite to human clinical trials. This approach would enable reduced numbers of animal experiments in line with the 3Rs principle and reduce associated development costs for early stage therapies.

Reviewer 1: Please clarify what clinical conditions this model is trying to simulate? Why did the authors prioritise catabolism over induction of defects?

Authors: The aim of the study was to develop a model mimicking the cellular, matrix and mechanical changes seen during human disc degeneration. These features are described in Table 1 and Fig. 1 and provide a range of effects, including loss of normal matrix, presence of cellular clusters, fissures and demarcation and cellular changes, including induction of catabolic enzymes, cytokines and factors that are known to regulate angiogenesis and nerve ingrowth in human disc degeneration.

Reviewer 1: Does this intervention allow for sufficient loosening of the collagenous network to enable injection of a hydrogel? How much volume?

Authors: As can be seen in the images of the whole disc in Fig. 4, cracks and fissures are induced within this model and, thus, we would predict that a similar volume for disc area would be able to be injected. When similar cracks have been seen in *in vivo* goat models, around 200-500 μL of hydrogels or other substances have been able to be injected. With naturally degenerate human discs, around 1-1.5 mL has been shown to be injected.

Reviewer 2: Please discuss advantages and limitations of this model. Specifically address similarities and differences between caprine, bovine and human IVDs with regards to size, diffusion distance, cell type and cell number. Also, please discuss treatment strategies that would be most suitable to be tested in the three species.

Authors: Bovine, caprine and human IVDs display similar cell types as they all lose the early NP progenitor cells (notochordal cells) early in development and, thus, are useful model systems to mimic human degeneration. Whilst bovine and caprine discs are generally smaller than lumbar human discs and more similar in size to human thoracic discs, with consequently reduced diffusion distances, cell numbers within caprine discs are similar to those seen in human discs. The use of bovine or caprine discs within model systems offers the advantage of a reduced variability between discs. Therefore, the model system described in the present study, which enables a reproducible moderate disc degeneration to be generated, will enable the exploration of new therapeutic options. This model could be utilised to perform *ex vivo* experiments and test treatment strategies targeting and modifying the IVD through gene, biological, cellular or biomaterial approaches or a combination thereof. Then, promising therapies could be further explored in whole human LDCS and *in vivo* animal models prior to clinical trials. The inclusion of the present model in the therapeutic development pipeline will enable fine tuning and targeting of therapies before progression to the clinic, reducing cost and increasing chance of success.

Editor's note: The Scientific Editor responsible for this paper was Mauro Alini.